Optimization of Receivers Field-of-Views in Multi-User VLC Networks: A Bio-inspired Approach

M W Eltokhey, Mohammad Ali Khalighi, Zabih Ghassemlooy

Optimization of Receivers Field-of-Views in Multi-User VLC Networks: A Bio-inspired Approach

M. W. Eltokhey, *Member, IEEE*, M. A. Khalighi, *Senior Member, IEEE*, Z. Ghassemlooy, *Senior Member, IEEE*

***Abstract*—Visible-light communication is a well known emerging technology, which enables high data rate wireless access in indoor environments, by making dual-use of light-emitting diode luminaires for providing lighting and communication. Managing the multiple access and addressing the users' mobility are among the current challenges of this technology. To manage the multiple-access interference arising from non-intended received signals of the other users, different approaches have been proposed so far, including zero-forcing pre-coding and broadcasting of the users' signals. However, by this approach, the network performance is sensitive to the users' locations, since they affect the correlation properties of the network channel matrix; a higher correlation (e.g., for the case of users getting closer together) results in a performance degradation. To mitigate this, we propose a novel approach of optimizing the receivers' field-of-views based on the bio-inspired particle swarm optimization, in order to adapt to the users' locations, and hence improve the network robustness. The efficiency of the proposed method is demonstrated through numerical simulations.**

***Index Terms*—Visible light communications; multiple-access interference; particle swarm optimization; ZF pre-coding; field-of-view optimization.**

I. Multi-user Visible-light Communication Networks

The ever-increasing bandwidth requirements to support the growing demand for high-speed data transmission in indoor scenarios, is overwhelming the radio frequency (RF) spectrum, which is already under a huge pressure. Subsequently, there has been a growing interest in the visible-light communication (VLC) technology during the past two decades, as a solution for broadband indoor communications. This has been driven by numerous advantages of this technology, such as utilizing the light-emitting-diode (LED) -based lighting infrastructure, operating at an unregulated frequency band, being unaffected by RF interference, and providing inherent security due to light confinement in most of the indoor environments [1].

One important requirement in VLC systems is ensuring coverage in large-space indoor environments. This can be realized through the use of multi-cell architectures, in the same way it is done in wireless RF cellular networks. This way, several LED luminaires will serve as access points (APs), which handle users within their respective illumination areas (cells). In such multi-cell VLC networks, which potentially should handle multiple users, each equipped with a receiver (Rx) that uses a photo-detector (PD), an important issue is to manage the multiple-access interference (MAI). In fact, MAI can arise from inter-user interference (IUI) or/and inter-cell interference (ICI), i.e., the received non-intended signals of the users in the same cell or/and in the other cells, respectively [2]. There has been a significant amount of research on the development of efficient multiple-access (MA) techniques for VLC networks so far [3]. The most popular solutions proposed include orthogonal frequency-division MA (OFDMA), non-orthogonal MA (NOMA), and pre-coded multi-user multiple-input single-output (MU-MISO) [4], [5]. Here, we focus on the third technique, i.e., pre-coded MU-MISO due to its implementation simplicity, suggesting it as a practical solution. There, a common approach is to use linear zero-forcing pre-coding (ZFPC) due to its simplicity and its good performance at relatively high signal-to-noise ratios (SNRs), which is mostly the case in indoor VLC networks, because of the short link distance in the case of unblocked line-of-sight (LOS) [6], [7].

The performance of ZFPC is largely affected by the locations of the users, as these determine the correlation between the users' channel gains [8]. In fact, a high correlation (e.g., due to nearly-located users) results in a degradation of the overall network performance. Although different Rxs' parameters can be optimized to improve the performance, one efficient solution for reducing this correlation is to appropriately tune the Rxs' field-of-views (FOVs), as proposed in [9], [10].

This article considers tuning of the Rxs' FOVs in MU-MISO ZFPC VLC systems to improve the network performance by decreasing the correlation in the network channel matrix. The novelty of the proposed method is that it relies on the "bio-inspired" algorithm of particle swarm optimization (PSO), which has been used in solving diverse problems in the area of optical wireless communications [11], [12]. We illustrate the advantages of this swarm intelligence technique in terms of efficiency and computational simplicity, and investigate the impact of varying the optimization parameters on the system performance. Also, we propose a solution to further reduce the computational complexity of the proposed optimization approach, and show its advantage in the case of user mobility.

In the sequel, we first describe the principles of a ZFPC VLC network. Next, we provide an overview of PSO and

M. W. Eltokhey and M. A. Khalighi are with Aix-Marseille University, CNRS, Centrale Marseille, Institut Fresnel, Marseille, France (e-mail: Mahmoud.Eltokhey@centrale-marseille.fr, Ali.Khalighi@fresnel.fr)

Z. Ghassemlooy is with Optical Communications Research Group, Faculty of Engineering and Environment, Northumbria University, Newcastle upon Tyne, NE1 8ST, UK (e-mail: z.ghassemlooy@northumbria.ac.uk)

This work has received funding from the European Union's Horizon 2020 research and innovation programme under the Marie Skłodowska-Curie grant agreement No. 764461 (VisIoN).

the proposed FOV tuning algorithm, before presenting the performance study of the proposed solution and discussing its practical implementation issues.

II. General Description of ZFPC VLC Networks

For VLC networks, the transmission link from the AP to the Rx is characterized mainly by the channel gain. We only account for the LOS path here. In fact, in the case of existing LOS in VLC networks, the contribution of non-LOS components is practically negligible [13]. The APs, i.e., the LED luminaires, are modeled by a Lambertian pattern of order m [13]. No lens is considered at the Rx, thus, the channel gain does not depend on the Rx's FOV.

Figure 1 illustrates the considered VLC network, with the main system blocks shown in Fig. 1(a). A central control unit coordinates between the APs for exchanging information (e.g., the channel state information, CSI), handling the ZFPC, as well as FOV optimization. To estimate the CSI at each Rx, pilot symbols are transmitted by the APs in the downlink. In the uplink, the estimated CSI are sent back to the APs using infrared links, for calculating the ZFPC matrix, and for FOV optimization.

To adjust the Rx's FOV, a mechanical iris is considered to be mounted on top of the plan of the PD's surface, to vary the maximum angle of reception at the Rx [14]. An illustration for the considered FOV tuning is presented in Figs. 1(b), 1(c), and 1(d).

We consider a MU-MISO broadcast VLC system, where N_t APs cooperate to serve N_r users, assuming $N_t \geq N_r$ [8], in order to comply with the ZFPC constraints. To manage the MAI, for instance, at AP_i, the desired signal of Rx_j, d_j, is multiplied by the pre-coding weight w_{ij}. We consider the max-min fairness criterion in [8] for calculating the ZFPC weights, due to it simplicity.

III. Particle Swarm Optimization

For optimization of the FOVs of the Rxs in the ZFPC system, we propose to use PSO, which mimics swarms movement [15]. Compared with other metaheuristic optimization techniques, the advantages of the PSO approach include its memory effect, in the sense that all particles acquire the knowledge of the good solutions in the solution space, because every particle shares its information with the others. In addition, PSO offers the advantages of a simple implementation and a relatively quick convergence, which are the reasons why it has received a great deal of attention in a wide range of applications. Consider a D-dimensional search space, which involves all possible combinations of the values of the D variables to be optimized. By PSO, within this search space, each point is a potential solution: each particle moves between points to find the optimal solution. The direction and the speed of the movements in the solution space are decided by the best solution found by the particle itself (personal best position, $Pbest$), and that found by the ensemble of particles (global best position, $Gbest$). The quality of these solutions is assessed using a fitness function designed according to the optimization goals.

PSO can be well described by an example of a swarm of bees (particles) searching in a garden (solution space) for location with most flowers (optimal solution), over a certain time (iterations). Bees communicate their experiences in terms of flowers' density at their locations to each other ($Pbest$ and $Gbest$), to decide the speed and direction of movement (particles' velocities) in their next move. The flowers' density corresponds to how good the location is (solution's quality), where higher flowers' densities correspond to better solutions. Figure 2 illustrates the considered PSO algorithm, where as shown in Figs. 2(a) and 2(b), particles (represented by bees) wander the 2-variable solution space formed by the axes of Variable 1 and Variable 2 to search for the optimal solution. The axis of fitness value represents the evaluation of each possible solution using the fitness function, where larger fitness values represent better solutions. In Fig. 2(a) the particles are distributed in the solution space and exchange information about the $Pbest$ and $Gbest$, which illustrates the exploration behaviour by the particles at the start of the optimization. Figure 2(b) shows the behavior of the particles at the last iterations, where they are about to converge to the optimal solution. A flow chart for the proposed FOV tuning algorithm using PSO is also shown in Fig. 2(c), where the dashed box at the right side depicts an example of two particles in a 3-dimensional solution space, illustrating the influence of the original velocity, $Pbest$, and $Gbest$ on the direction and the velocity of the particles' movements. Figure 2(d) illustrates the idea of reducing the correlation in the network channel matrix by optimization of the FOVs, highlighting the impact of varying the Rx FOV using PSO on the channel gains at the Rxs, and subsequently the ZF pre-coding network performance.

The main parameters of the PSO algorithm include the maximum number of iterations N_{it}, the number of particles N_p, and the number of variables D. For updating the velocities and the positions of the particles, the approach in [11] is considered. Without loss of generality, for preventing particles from moving to locations outside the solution space, hard boundary conditions are considered here, where new positions (represented by new variables' values) exceeding the solution space are clipped, in order to remain at the boundaries.

IV. FOV Tuning Using PSO

Here, we describe the proposed FOV tuning algorithm. As shown in Fig. 2(c), the algorithm starts with generating for each particle (i.e., possible solution, represented by a set of FOVs for all Rxs) random positions (sets of FOVs) and velocities (rates of varying of the tested sets of FOVs in the solution space), prior to evaluating in each step (iteration) the performance of each particle and updating them. To evaluate the performance of a particle (the quality of the solution formed by a particular set of FOVs), the corresponding solution is converted from integer values to FOVs, which are forwarded to the Rxs in the downlink to apply them. Note that, to generalize the proposed algorithm to the cases where only discrete non-equally-separated FOV values are possible (e.g., FOVs $\in [10^\circ, 30^\circ, 40^\circ]$), the possible FOV values are

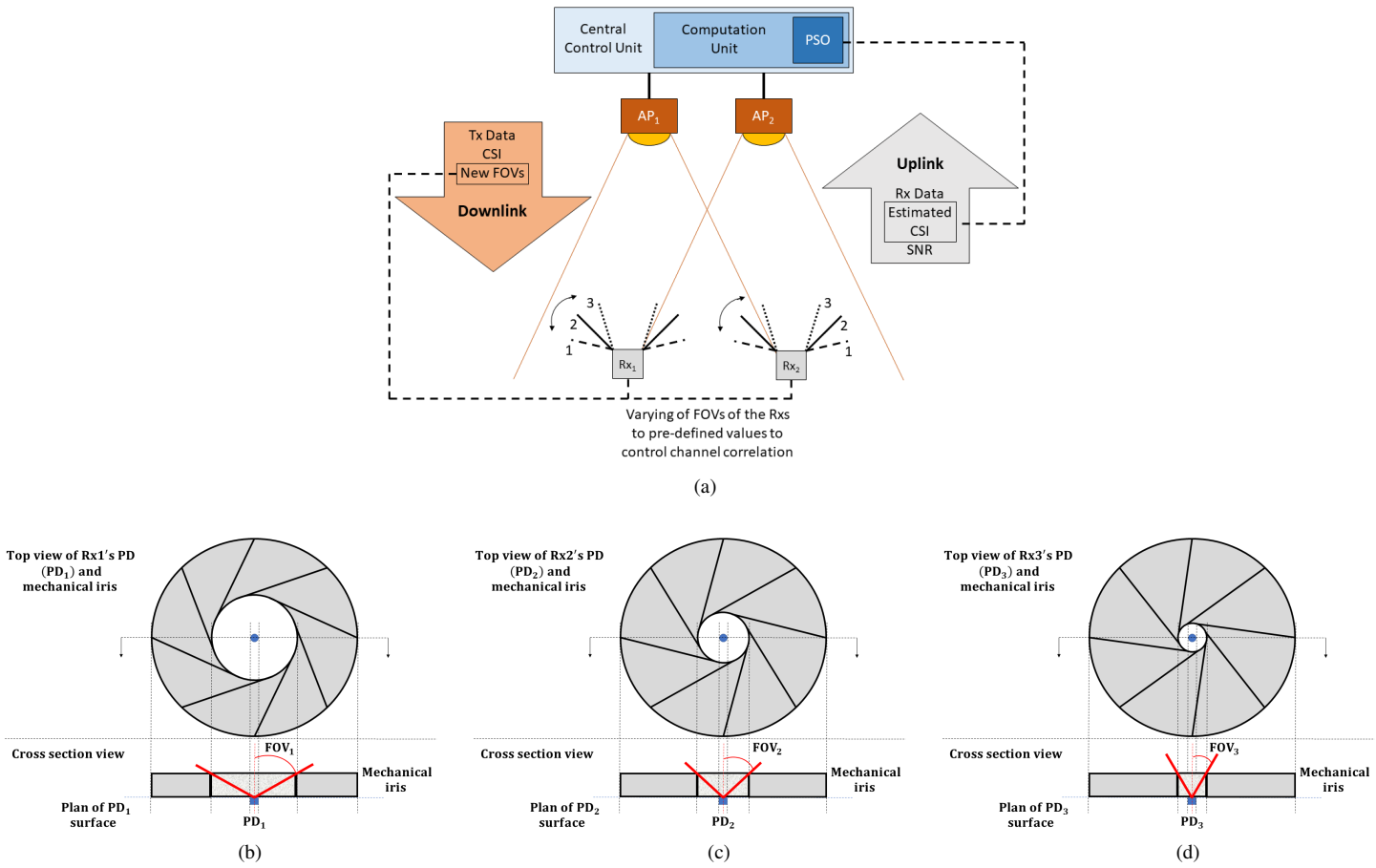

Fig. 1: FOV tuning in the VLC network. (a): main blocks in the VLC system. (b), (c), (d): Examples of FOV tuning using mechanical iris for three Rxs, where $\text{FOV}_1 > \text{FOV}_2 > \text{FOV}_3$.

converted to integer values, and the problem is solved as an integer programming problem. In particular, the indices of the FOVs (in ascending order of FOVs) are used as the values in the solution space, to ensure equal spacing between the possible FOVs.

The proposed approach is illustrated in Fig. 2(d), where in the downlink, the central control unit sends to the Rxs (via the APs) the calculated FOVs, as shown in Fig. 1(a). Next, the estimated channel gains at the Rxs (i.e., the elements of the network channel matrix) using these FOVs are sent back in the uplink to the central control unit to update the FOVs using PSO. Based on these evaluations, and after updating the positions and velocities of the particles and the system experience, i.e., $Pbest$ and $Gbest$, PSO continues searching new FOVs that achieve a better performance by exploring possible better solutions. Once the maximum number of iterations is achieved, the $Gbest$ is considered as the solution corresponding to the optimized FOVs. As shown in Fig. 1(a), the additional overhead only concerns the optimized FOVs in the downlink, and the SNR performance in the uplink, which remain very limited. Note that, given the limited users' mobility in indoor scenarios, the variations in the network channel matrix are relatively slow, which relaxes the adaptation requirements, and the constraints on the delay from the feedback channel.

A mechanical iris is used at the top of each PD to tune the corresponding Rx's FOV. To consider a practical design, we assume that the FOVs can be only tuned to discrete values, ranging between $10°$ and $80°$, with a step of $5°$. Note that the speed of variation of the FOV highly depends on the parameters of the mechanical iris, as well as on the tools used for controlling it, which is beyond the scope of this optimization study. Note that, the relatively slow changes of the channel in indoor scenarios would justify the neglected delay in the adjustment of the parameters of the mechanical iris. To evaluate the solution of PSO for FOV tuning, we propose to consider the following fitness function:

$$\text{Fitness} = F_1 \times \sum_{j=1}^{N_r} R_j - F_2 \times \text{cond}(\boldsymbol{H}) - (F_3 \times N_0), \quad (1)$$

where $\text{cond}(\boldsymbol{H})$ refers to the 2-norm condition number of the network channel matrix $\boldsymbol{H}$, R_j denotes the data-rate of the user j, and N_0 is defined as the number of users with no existing LOS link with any AP. Also, F_1, F_2, and F_3 are the weights given to the 1st, 2nd, and 3rd terms of the fitness function, respectively. In fact, the 1st term ensures promoting solutions with higher sum-rates (i.e., the total achievable network throughput), the 2nd term downgrades solutions resulting in high condition number for network channel matrix, and the 3rd term guarantees that the solutions resulting in users

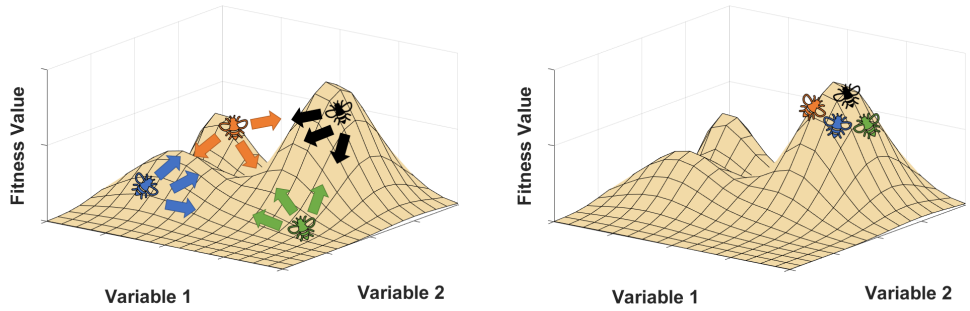

(a) (b)

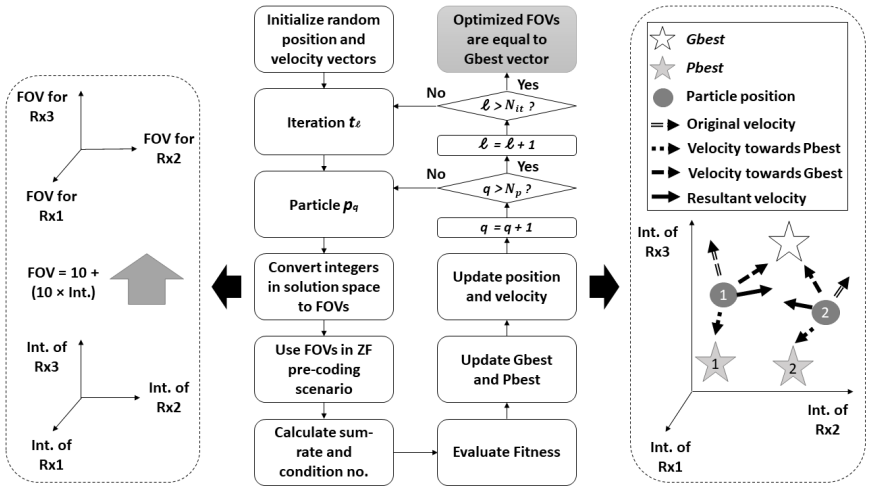

(c)

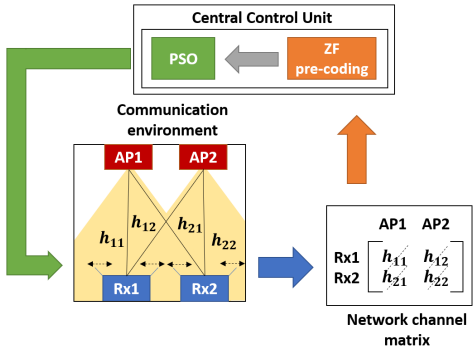

(d)

Fig. 2: PSO algorithm description. (a), (b): Illustrations of particles at the first (exploring the solution space while exchanging information) and last (about to converge to the optimal solution) iterations, respectively. (c): Flow chart of the algorithm for an example of optimizing the FOVs of 3 Rxs, indices ℓ and q refer to the iteration number and the particle number, respectively, "Int." stands for integer. Dashed box at the left side shows how the variable values (FOVs) are extracted from integers during the optimization to solve the problem as integer programming problem, for a generalized solution in cases of having non-uniform steps between the possible FOVs. Dashed box at the right side illustrates an example of behavior of 2 particles, under the influence of original velocity, $Pbest$, and $Gbest$. (d): Illustration of the proposed FOV optimization for the case of two APs and two Rxs: By tuning the FOVs, the entries of the network channel matrix are controlled; h_{ij} denotes the channel gain of the communication link between AP_i and Rx_j.

with LOS blockage are excluded. This is done by giving F_3 a large value, so that for any value of the sum-rate and condition number achieved by a solution, having a user with no LOS results in a bad evaluation of the solution. This point is explained in more detail in the next section. Note that, due to the non-linear nature of the considered problem, any variation in the Rxs' locations requires re-adapting the model to have FOVs that satisfy LOS coverage. This makes PSO more suitable compared to other techniques which require training data to update the model adaptively depending on the actual LOS coverage conditions.

V. Performance Analysis

This section presents numerical results, for comparing the network performance for the cases of non-optimized FOVs and optimized FOVs using PSO. Consider four Rxs in the VLC network, handled by ZFPC. All Rxs are assumed to point up to the ceiling. Four LED luminaires (APs) are assumed, connected to a central control unit. The indoor environment is considered of dimension $(7 \times 7 \times 3)\,\mathrm{m}^3$, while the APs are located at (x, y, z) positions (2.25, 2.25, 2.5), (2.25, 4.75, 2.5), (4.75, 2.25, 2.5), and (4.75, 4.75, 2.5). The number of LED chips per luminaire is 36, the current per luminaire is $3.6\,\mathrm{A}$, the Lambertian order m of each LED is 1, and the LED conversion efficiency $\mathcal{S}$ is 0.44 W/A [2]. The noise power spectral density is fixed to $10^{-21}\,\mathrm{A}^2$/Hz, and the considered PD responsivity and area are $0.4\,\mathrm{A/W}$ and $1\,\mathrm{cm}^2$, respectively [2].

The network sum-rate (corresponding to the 1st term in (1)) is calculated for a system bandwidth of 10 MHz, assuming DC-biased optical-orthogonal frequency-division multiplexing (DCO-OFDM) signal modulation. Also, the 2-norm condition numbers in the considered random user positions (corresponding to the 2nd term in (1)) reached orders of 10^3. Following the discussions at the end of the previous section, we hence set the constants F_1, F_2, and F_3 in (1) to 1, 10^5, and 10^{10}, respectively, to guarantee that the 3rd term in (1) is always dominating, and to further ensure that the solutions with very large 2-norm condition numbers are downgraded. In addition, to further downgrade the solutions with LOS blockage, we set the corresponding network sum-rates to zero.

A. Performance over different optimization parameters

To choose the best combination of particles and iterations for a given total number of evaluations of $N_p \times N_{it}$, Table I compares the average network sum-rate and the number of LOS blockage cases for different values of N_p and N_{it}, for 1000 random user positions with random Rxs' heights Z_{Rx} between 0.85 and $1.35\,\mathrm{m}$. The 1000 random positions are picked from 1250 random positions, with random elevation and azimuth angles for the Rxs' within the range of (0°-45°) and (0°-180°), respectively, such that they guarantee LOS coverage at the Rxs' FOVs of $80°$. This ensures the feasibility of using the proposed optimization in finding optimized solutions, given that each of the optimized FOVs has a maximum value of $80°$. The sum-rate is averaged over all users' positions corresponding to LOS coverage occurrence. Note that, *LOS blockage* refers to the cases where one or more Rxs have no LOS path with any AP. Obviously, a lower LOS blockage indicates a better LOS coverage probability. A LOS blockage of 0 indicates that there has been no LOS blockage over the considered random scenarios, which is generally the case due to a better exploration of the solution space.

TABLE I: Comparison between different combinations of number of particles (N_p) and iterations (N_{it}) over average sum-rate and LOS blockage performance, for cases of random Rx heights in 4 Rx scenarios.

Combination	Av. sum-rate (bps) $\times 10^7$	LOS blockage
N_p = 5, N_{it} = 10	4.19	25
N_p = 10, N_{it} = 5	4.27	3
N_p = 10, N_{it} = 10	4.42	2
N_p = 10, N_{it} = 20	4.50	0
N_p = 20, N_{it} = 10	4.60	0

Given the considered 15 possible FOVs for the Rxs, the number of evaluations required for a "parameter sweep" (i.e., trying all possible combinations of FOVs for finding optimum values, without using an optimization algorithm) for scenarios with 2, 3, and 4 Rxs, are 225, 3375, and 50625, respectively. Obviously, the considered numbers of evaluations $N_p \times N_{it}$ in Table I are much smaller than those needed for a parameter sweep.

As can be seen, increasing the number of evaluations from 50 to 100, and from 100 to 200, results in an improved performance in terms of average sum-rate and LOS blockage, as expected. In addition, it is noted from the cases with 50 or 200 evaluations that, having a larger number of particles than iterations (for the same number of evaluations) results in a better average sum-rate, and a lower LOS blockage (in case of 50 evaluations). This can be explained by the better exploration of the solution space before converging to the optimal solution.

B. Case study of optimized and non-optimized FOVs

To show in more detail how the FOVs and the sum-rate performance vary over iterations throughout the proposed optimization, we consider in Fig. 3 the performance of a certain scenario, where 4 Rxs with height of $0.85\,\mathrm{m}$ are located at (x, y) of (4.58, 0.32), (5.08, 4.03), (3.63, 5.47), and (1.49, 1.58). Figure 3(b) shows the fitness function calculated using (1) at each iteration. In the blue boxes, are indicated the FOVs, the sum-rates, and the condition numbers of $\boldsymbol{H}$ at every change of the fitness value, representing the most optimal performance achieved at that iteration. Also, the red boxes indicate the sum-rates achieved in cases of fixed FOVs of 50°, 70°, and 90°. The plot shows an improvement in the quality of the solution due to the further exploration of the solution space, where PSO converges to the optimal solution at iteration 6.

We note from the data provided in the red boxes that decreasing the FOV in general should improve the performance, however, this remains dependent on the correlation of the network channel matrix. This can be verified from the slight decrease in the 2-norm condition number and the small increase in the network sum-rate by increasing the FOV from 70° to 90°. This elucidates the complexity of the problem, and the fact that the sum-rate performance is not always improved by simply decreasing the FOVs.

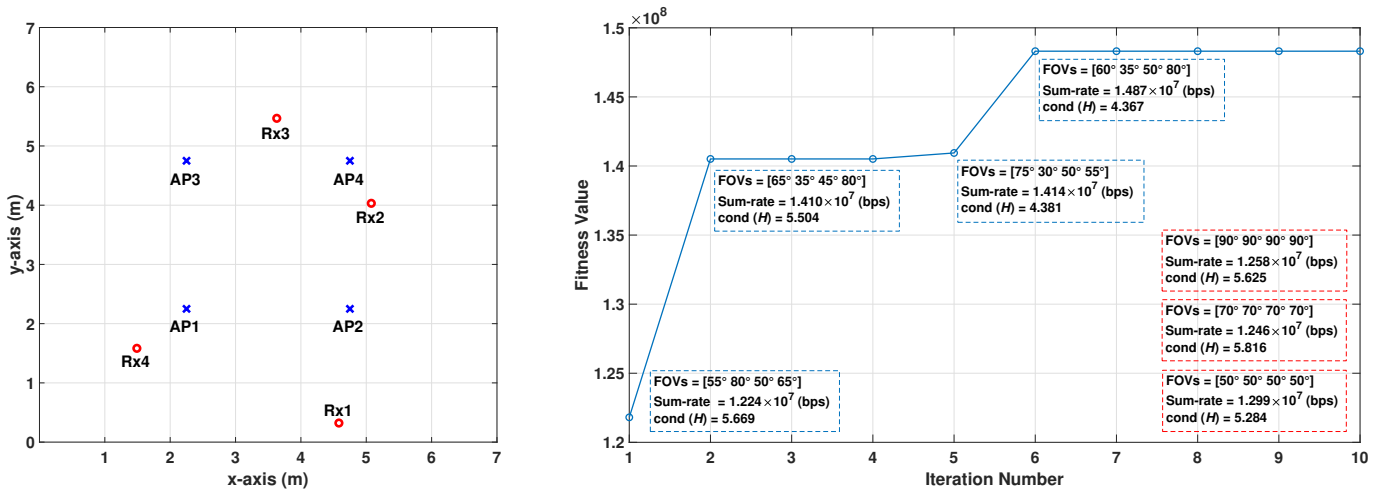

(a) (b)

Fig. 3: Comparison between optimized and non-optimized FOVs for a 4 Rx - 4 AP scenario. (a): Top view for the locations of the Rxs and the APs with heights of 0.85 m and 2.5 m, respectively. (b): Fitness value versus optimization's iterations. The dashed blue boxes represent the optimized FOVs over changes in fitness and their corresponding sum-rates. The dashed red boxes correspond to the non-optimized FOVs (50°, 70°, and 90°).

C. Performance over random Rx locations

Using the best combination of N_p and N_{it} from Table I (i.e., $N_p = 20$ and $N_{it} = 10$), we compare in Table II the LOS blockage occurrence and the average sum-rate for the cases of non-optimized and optimized FOVs for 4 Rxs. Comparison is carried out over 1000 random scenarios. Non-optimized FOV values of 50°, 60°, 70°, 80°, and 90° are considered, however, the results of LOS blockage for FOVs of 80° and 90° were excluded from the table as all Rxs have LOS coverage over all scenarios. For the same reason of LOS blockage, the average sum-rate results for FOVs of 50°, 60°, and 70° were excluded.

It is observed that increasing the FOV decreases the risk of LOS blockage. However, in general, this comes at the expense of increased homogeneity between users' channel gains, thus a performance degradation due to higher probability of increased correlation in the network channel matrix (which is apparent only for the highly constrained case of random Rxs' orientations for the large FOVs of 80° and 90°). Also, considering random Rxs' orientations in addition to random Rxs' heights led to a degraded sum-rate performance, due to lower number of solutions that satisfy LOS coverage. Moreover, increasing the Rx's height (i.e., decreasing the path length between the Tx and the Rx) increases the probability of LOS blockage, due to the decrease in the area covered on the AP plane by the Rx's FOV. On the other hand, irrespective of the considered Rxs' heights, the proposed FOV optimization shows a robust performance, with very limited LOS blockage occurrence. It is worth mentioning that, even by decreasing the number of evaluations to 50 (see Table I), the achieved performance with PSO was still better than the cases with non-optimized FOVs.

Similar observations can be made by considering the network average sum-rate, where the proposed approach outperforms the case of non-optimized FOVs. This advantage results from the adaptation of every Rx to users' positions to decrease the correlation in the network channel matrix. Increasing the Rxs' heights results in an average sum-rate degradation, because of higher correlation between users' channel gains, as a result of shorter transmission path lengths.

TABLE II: Number of scenarios with at least 1 Rx with no LOS coverage and average sum-rate performance for optimized (Opt.) and non-optimized fixed FOVs, for fixed and random Z_{Rx} between 0.85 and 1.35 m, and random Rxs' orientations.

	LOS blockage			
FOV	$Z_{Rx} = 0.85$ m	$Z_{Rx} = 1.15$ m	Random Z_{Rx}	Random orientations
50°	668	873	840	786
60°	30	268	257	491
70°	0	0	0	194
Opt.	0	0	0	15
	Average sum-rate (bps) $\times 10^7$			
80°	3.24	3.06	3.10	3.06
90°	3.24	3.06	3.10	2.88
Opt.	5.18	4.50	4.60	4.46

D. Performance in the case of user mobility

To further decrease the number of evaluations in the case of changing users' positions, we propose to forward the most recent optimized FOVs as initial positions for PSO, for a faster convergence. To prevent particles from converging to sub-optimal solutions because of insufficient exploration of the solution space, we propose to vary these initial values by a random factor between 0 and 50% for each particle, in order to increase the spread of the particles in the solution space. We refer to this approach as "memory-assisted" optimization. The efficiency of this approach was investigated on 1000 scenarios generated by the random way-point model, simulating the mobility of 4 Rxs with velocities varying between 0.1 and 0.5 m/sec, and a time interval of 5 sec between two successive

TABLE III: LOS blockage and average sum-rate performance for different cases of optimized and non-optimized FOVs for 1000 generated positions of 4 Rxs reflecting user mobility according to random way-point model.

	Non-optimized	Memory-assisted PSO (N_p = 10)		Conventional PSO (N_p = 10)	
Z_{Rx}	FOV = 80°	N_{it} = 5	N_{it} = 10	N_{it} = 5	N_{it} = 10
LOS blockage					
0.85 m	0	0	0	1	0
1.15 m	0	0	0	3	2
Average sum-rate (bps) $\times 10^7$					
0.85 m	2.92	4.20	4.36	4.43	4.58
1.15 m	2.76	3.74	3.86	3.84	3.97

positions. The comparison is carried out over Rxs' heights of $0.85\,\text{m}$ and $1.15\,\text{m}$, and for different numbers of particles and iterations.

Table III shows a comparison of the average sum-rate and the LOS blockage performance between the cases of conventional and memory-assisted PSO-based FOVs' optimization, as well as the case of fixed FOV of $80°$. This latter corresponds to the best performance for non-optimized FOVs, as seen in Table II. The results show a quite robust LOS blockage performance for the memory-assisted approach, compared with the conventional optimization. As before, for the case of conventional optimization, LOS blockage occurrence improves with increasing the number of evaluations from 50 to 100 or by decreasing the Rxs' heights. For the average sum-rate, both conventional and memory-assisted optimizations outperform the non-optimized case, while decreasing the Rxs' heights or increasing the number of evaluations results in an improved performance. However, we notice that the conventional optimization provides a better average sum-rate performance, which can be explained by a more constrained exploration of the solution space in the case of memory-assisted optimization. Indeed, the initial values are not distributed over the entire solution space as it is the case for conventional optimization. Lastly, concerning the computational complexity, for each particle and at each iteration, the proposed PSO-based optimization needs to (i) update the velocities, calculate the fitness function, and enforce the boundary conditions; and (ii) calculate the ZFPC solution.

VI. Conclusions

We proposed in this article the optimization of the Rxs' FOVs based on PSO, for ZFPC MU-MISO VLC networks. Firstly, we highlighted the trade-off between the solution quality and the number of evaluations, and showed that using a sufficient number of particles is essential for an adequate exploration of the solution space. In general, decreasing the FOV improves the average sum-rate but it also increases the risk of LOS blockage. The proposed optimized FOV tuning approach offers the best trade-off between a good throughput performance and a robust LOS coverage. The performance of optimized and non-optimized FOVs were also compared in the case of user mobility, where it was shown that by using the last optimized FOVs as initial values for the PSO, a better LOS blockage performance is achieved using a smaller number of evaluations. However, this comes at the expense of a slightly lower average sum-rate, due to the constrained exploration of the solution space. Nevertheless, the robust performance achieved with a limited number of evaluations, makes this approach suitable for the cases of limited computational resources or relatively high user mobility. For scenarios with still more constrained computational resources, the optimization of FOVs can be carried out only in cases where the channel correlation exceeds a certain threshold.

Given the promises of the proposed scheme in improving the network performance, future research could investigate the merits of this approach while taking into account the practical constraints.

This includes, for instance: investigation of other pre-coding schemes (i.e., other than ZF pre-coding); consideration of the user mobility, random tilting of the Rxs, and parameters of the mechanical iris used for controlling the FOVs including the required delay for FOV tuning; optimization of the FOV with the lowest possible number of changes to ensure minimum delay; and improvement of the proposed memory-assisted optimization to increase the solution quality by controlling the impact of the most recent optimized FOVs.

Note that the proposed approach for FOV optimization can be applied to other areas in the field of wireless communications that require real-time adaptation to changing network configuration, where the presented study, in particular, concerning the consideration of the constraints on the possible values in the solution space, the trade-off between the PSO parameters, and the design of the fitness function, can be quite insightful.

References

[1] Z. Ghassemlooy, L. N. Alves, S. Zvanovec, and M. A. Khalighi, Eds., *Visible Light Communications: Theory and Applications*. CRC-Press, 2017.

[2] M. W. Eltokhey, M. A. Khalighi, A. S. Ghazy, and S. Hranilovic, "Hybrid NOMA and ZF pre-coding transmission for multi-cell VLC networks," *IEEE Open Journal of the Communications Society*, vol. 1, pp. 513–526, 2020.

[3] S. Al-Ahmadi, O. Maraqa, M. Uysal, and S. M. Sait, "Multi-user visible light communications: State-of-the-art and future directions," *IEEE Access*, vol. 6, pp. 70 555–70 571, 2018.

[4] M. W. Eltokhey, M. A. Khalighi, and Z. Ghassemlooy, "Multiple access techniques for large space indoor scenarios: A comparative study,," in *International Conference on Telecommunications (ConTEL)*, July 2019, Graz, Austria.

[5] I. Abdalla, M. B. Rahaim, and T. D. Little, "Interference in multi-user optical wireless communications systems," *Philosophical Transactions of the Royal Society A*, vol. 378, no. 2169, 2020.

[6] T. V. Pham, H. L. Minh, and A. T. Pham, "Multi-cell VLC: Multi-user downlink capacity with coordinated precoding," in *2017 IEEE International Conference on Communications Workshops (ICC Workshops)*, May 2017, pp. 469–474, Paris, France.

[7] Z. Feng, C. Guo, Z. Ghassemlooy, and Y. Yang, "The spatial dimming scheme for the MU-MIMO-OFDM VLC system," *IEEE Photonics Journal*, vol. 10, no. 5, pp. 1–13, Oct. 2018.

[8] Z. Yu, R. J. Baxley, and G. T. Zhou, "Multi-user MISO broadcasting for indoor visible light communication," in *International Conference on Acoustics, Speech and Signal Processing (ICASSP)*, May 2013, pp. 4849–4853, Vancouver, Canada.

[9] Y. Hong, J. Chen, Z. Wang, and C. Yu, "Performance of a precoding MIMO system for decentralized multiuser indoor visible light communications," *IEEE Photonics Journal*, vol. 5, no. 4, pp. 7 800 211–7 800 211, Aug. 2013.

[10] H. Marshoud, D. Dawoud, V. M. Kapinas, G. K. Karagiannidis, S. Muhaidat, and B. Sharif, "MU-MIMO precoding for VLC with imperfect CSI," in *2015 4th International Workshop on Optical Wireless Communications (IWOW)*, Sep. 2015, pp. 93–97, Istanbul, Turkey.

[11] M. W. Eltokhey, K. R. Mahmoud, Z. Ghassemlooy, and S. S. Obayya, "Optimization of intensities and locations of diffuse spots in indoor optical wireless communications," *Optical Switching and Networking*, vol. 33, pp. 177 – 183, 2019.

[12] M. S. Demir, S. M. Sait, and M. Uysal, "Unified resource allocation and mobility management technique using particle swarm optimization for VLC networks," *IEEE Photonics Journal*, vol. 10, no. 6, pp. 1–9, 2018.

[13] S. Long, M. A. Khalighi, M. Wolf, S. Bourenanne, and Z. Ghassemlooy, "Investigating channel frequency selectivity in indoor visible light communication systems," *IET Optoelectronics*, vol. 10, no. 3, pp. 80–88, May 2016.

[14] I. Abdalla, M. B. Rahaim, and T. D. C. Little, "Dynamic FOV visible light communications receiver for dense optical networks," *IET Communications*, vol. 13, no. 7, pp. 822–830, 2019.

[15] J. Kennedy and R. Eberhart, "Particle swarm optimization," in *Proceedings of ICNN'95 - International Conference on Neural Networks*, vol. 4, Nov. 1995, pp. 1942–1948 vol.4, Perth, Australia.